Escherichia coli Biotin Synthase Produces Selenobiotin. Further Evidence of the Involvement of the [2Fe-2S]$^{2+}$ Cluster in the Sulfur Insertion Step†

Bernadette Tse Sum Bui,*,‡ Tony A. Mattioli,§ Dominique Florentin,‡ Gérard Bolbach,‡ and Andrée Marquet*,‡

Université Pierre et Marie Curie-Paris6, UMR CNRS 7613, Paris F-75005, France, Synthèse, Structure et Fonction de Molécules Bioactives, and Laboratoire de Biophysique du Stress Oxydant, SBE/DBJC, CNRS URA 2096, CEA/Saclay, 91191 Gif-sur-Yvette Cedex, France

Received November 22, 2005; Revised Manuscript Received January 25, 2006

ABSTRACT: Biotin synthase, a member of the "radical SAM" family, catalyzes the final step of the biotin biosynthetic pathway, namely, the insertion of a sulfur atom into dethiobiotin. The as-isolated enzyme contains a [2Fe-2S]$^{2+}$ cluster, but the active enzyme requires an additional [4Fe-4S]$^{2+}$ cluster, which is formed in the presence of $Fe(NH_4)_2(SO_4)_2$ and Na_2S in the in vitro assay. The role of the [4Fe-4S]$^{2+}$ cluster is to mediate the electron transfer to SAM, while the [2Fe-2S]$^{2+}$ cluster is involved in the sulfur insertion step. To investigate the selenium version of the reaction, we have depleted the enzyme of its iron and sulfur and reconstituted the resulting apoprotein with $FeCl_3$ and Na_2Se to yield a [2Fe-2Se]$^{2+}$ cluster. This enzyme was assayed in vitro with Na_2Se in place of Na_2S to enable the formation of a [4Fe-4Se]$^{2+}$ cluster. Selenobiotin was produced, but the activity was lower than that of the as-isolated [2Fe-2S]$^{2+}$ enzyme in the presence of Na_2S. The [2Fe-2Se]$^{2+}$ enzyme was additionally assayed with Na_2S, to reconstitute a [4Fe-4S]$^{2+}$ cluster, in case the latter was more efficient than a [4Fe-4Se]$^{2+}$ cluster for the electron transfer. Indeed, the activity was improved, but in that case, a mixture of biotin and selenobiotin was produced. This was unexpected if one considers the [2Fe-2S]$^{2+}$ center as the sulfur source (either as the ultimate donor or via another intermediate), unless some exchange of the chalcogenide has taken place in the cluster. This latter point was seen in the resonance Raman spectrum of the reacted enzyme which clearly indicated the presence of both the [2Fe-2Se]$^{2+}$ and [2Fe-2S]$^{2+}$ clusters. No exchange was observed in the absence of reaction. These observations bring supplementary proof that the [2Fe-2S]$^{2+}$ cluster is implicated in the sulfur insertion step.

Biotin synthase (BS),[1] a member of the "radical SAM" family (*1*), catalyzes the final step of the biotin biosynthetic pathway, namely, the insertion of a sulfur atom into dethiobiotin (DTB) (Scheme 1) (*2*−*4*).

Selenobiotin is a natural substance which has been characterized as an excretion product of the fungus *Phycomyces blakesleeanus* (*5*), and one would expect that it has been produced by biotin synthase, using the same mechanism. We decided to investigate this reaction in vitro.

A consistent picture is now emerging for the *Escherichia coli* biotin synthase mechanism. The as-isolated enzyme is a homodimer and contains one air-stable [2Fe-2S]$^{2+}$ cluster per monomer (*6*−*8*). Reconstitution of this form under strictly anaerobic conditions, in the presence of dithiothreitol (DTT) and an excess of Fe^{3+} and Na_2S, gives rise to an additional air-sensitive [4Fe-4S]$^{2+}$ cluster (*8*, *9*), located at a separate site, as determined by Mössbauer spectroscopy (*10*). The crystal structure of reconstituted BS in the presence of DTB and *S*-adenosylmethionine (SAM or AdoMet) has been determined and shows indeed the presence of these two distinct clusters at different sites in the protein (*11*). This mixed cluster state is essential for optimal activity, and each

Scheme 1: Reaction Catalyzed by Biotin Synthase

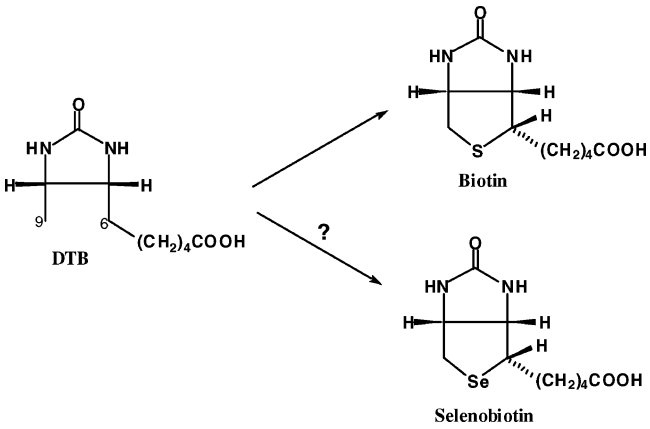

† This research has been supported in part by the European Community's Human Potential Programme under Contract HPRN-CT-2002−00244 (Viteomics).

* To whom correspondence should be addressed. B.T.S.B.: telephone, +33 1 44 27 31 13; fax, +33 1 44 27 71 50; e-mail, tsesum@ccr.jussieu.fr. A.M.: telephone, +33 1 44 27 31 13; fax, +33 1 44 27 71 50; e-mail, marquet@ccr.jussieu.fr.

‡ UMR CNRS 7613.

§ CEA Saclay CNRS URA 2096.

[1] Abbreviations: AdoMet or SAM, *S*-adenosylmethionine; BS, biotin synthase; 5-DAF, 10-methyl-5-deazaisoalloxazine; $AdoCH_2^{\cdot}$, 5′-deoxyadenosyl radical; DTB, dethiobiotin; DTT, dithiothreitol; EDTA, ethylenediaminetetraacetic acid; HPLC, high-pressure liquid chromatography; [Fe-S] cluster, iron−sulfur cluster; [Fe-Se] cluster, iron−selenium cluster; NADPH, nicotinamide adenine dinucleotide phosphate, reduced form; TFA, trifluoroacetic acid; Tris-HCl, tris(hydroxymethyl)aminomethane hydrochloride.

10.1021/bi052388m CCC: $33.50
Published on Web 02/28/2006

cluster plays a unique chemical role in the catalytic mechanism. It is now clear that the $[4Fe\text{-}4S]^{2+}$ center, common to all radical SAM enzymes (*12*−*14*), mediates the transfer of one electron from NADPH to AdoMet, via flavodoxin reductase (*15*) and flavodoxin (*16*). This generates methionine and the deoxyadenosyl radical ($AdoCH_2^{\bullet}$) (*17*−*19*). The deoxyadenosyl radical then abstracts a hydrogen at C-9 of dethiobiotin (*20*), and the resulting $DTB^{\bullet}$ radical then quenches a sulfur atom. Evidence exists for the participation of the $[2Fe\text{-}2S]^{2+}$ cluster in the sulfur insertion step (*7*, *21*−*23*), giving an intermediate whose chemical nature has not yet been defined. A second $AdoCH_2^{\bullet}$ radical is generated from another AdoMet (*20*), producing a radical at C-6 of this intermediate, ending in ring closure. Another hypothesis has postulated a cysteine desulfurase activity for biotin synthase, leading to an intermediate protein-bound persulfide which acts as the sulfur donor (*24*). However, the experimental data could not be reproduced by several groups, as discussed previously (*25*).

To investigate the selenium version of the reaction, it was necessary to replace both [Fe-S] centers of biotin synthase with [Fe-Se] centers. The preparation of apo-biotin synthase by treatment of the native $[2Fe\text{-}2S]^{2+}$ form, either with sodium dithionite (*7*, *26*, *27*) or with photoreduced 10-methyl-5-deazaisoalloxazine (5-DAF) (*25*, *28*), has been described previously. We and others have previously shown that a $[2Fe\text{-}2S]^{2+}$ center identical to the one present in the as-isolated form can be reconstituted when the apoenzyme was incubated with $FeCl_3$, Na_2S, and DTT in Tris buffer in the presence of traces of oxygen. In this case, the reconstituted enzyme exhibited the same UV−visible (*7*), Mössbauer (*26*), and resonance Raman (*8*) spectra and activity (*7*) as the as-isolated one under the standard assay conditions.

We have also already described the reconstitution of a $[2Fe\text{-}2Se]^{2+}$ center in the apoenzyme using selenocystine and NifS as a source of Se^{2-}. The selenoenzyme was characterized by its Fe and Se contents and by UV−visible and circular dichroism spectroscopy (*27*). Some activity, as measured by the paper disc-plate method using *Lactobacillus plantarum* (*29*), was observed, but the reaction products were not characterized. In the work presented here, we used pure, chemically synthesized Na_2Se (*30*), to precisely control the Se^{2-} concentration during the reconstitution and enzymatic assay. The resulting $[2Fe\text{-}2Se]^{2+}$ center was further characterized by resonance Raman spectroscopy, a vibrational technique which is well suited to distinguishing between [Fe-S] and [Fe-Se] clusters (*31*), due to the large atomic mass differences between sulfur and selenium.

Using the classical in vitro assay conditions (*25*), by just replacing Na_2S with Na_2Se, we anticipated the formation of an additional $[4Fe\text{-}4Se]^{2+}$ center. With this system, selenobiotin was indeed formed, but the activity was much lower than that of the $[2Fe\text{-}2S]^{2+}$ enzyme in the presence of Na_2S. When this $[2Fe\text{-}2Se]^{2+}$ enzyme was incubated with Na_2S instead of Na_2Se (assuming that we would form a mixture of $[2Fe\text{-}2Se]^{2+}$ and $[4Fe\text{-}4S]^{2+}$ clusters, with the $[4Fe\text{-}4S]^{2+}$ cluster being more efficient for electron transfer), the activity was improved. HPLC analysis of the supernatant revealed a mixture of biotin and selenobiotin. This was unexpected if the $[2Fe\text{-}2S]^{2+}$ center is the sulfur donor, unless some exchange of the chalcogenide has taken place in this cluster. Analysis of the resonance Raman spectrum of the reacted enzyme indicates that this is the case, whereas no exchange was observed in the absence of reaction.

MATERIALS AND METHODS

Materials. Chemicals were purchased from either Sigma-Aldrich Chemical Co., VWR International, or Acros Organics unless otherwise stated. Selenobiotin was available in our laboratory (*32*). Sodium selenide (*30*) was prepared as follows. Selenium powder (200 mg, 2.53 mmol) was added to NaOH (563 mg) and sodium formaldehyde sulfoxylate (713 mg), dissolved in argon-saturated water (2.5 mL). After the mixture had been stirred at 60 °C for 1 h, a white precipitate appeared. This mixture was cooled to 0 °C and then transferred into a glovebox (Jacomex BS531 NMT) equipped with an oxymeter (ARELCO ARC), filled with a nitrogen atmosphere containing <2 ppm oxygen. The sodium selenide was filtered through a filter paper (No. 00) and left to dry for a few days before addition of 20 mL of 50 mM Tris (pH 8) (hereafter termed "buffer"). The real concentration of the stock solution of Na_2Se was determined as described elsewhere (*33*), by converting Na_2Se into PbSe; 0.125 mL of various estimated concentrations of Na_2Se (0.1, 0.2, 0.5, and 1 mM; assuming quantitative conversion of Se to Na_2Se) was added to 0.875 mL of a solution of 5 mM lead acetate dissolved in 0.1 N HCl in a spectrophotometric cuvette. The absorbance of the yellowish-brown PbSe solution was immediately measured at 400 nm by using a molar coefficient for PbSe of 1.18×10^4 cm^{-1} M^{-1}. The exact concentration of the stock solution of Na_2Se was found to be 108 mM, indicating that the yield of the synthesis of Na_2Se was 85%. This solution was kept inside the glovebox, and its concentration remained constant over a long time period, showing that Na_2Se was stable under an inert atmosphere.

Bacterial Strains and Enzyme Purification. Preparations of flavodoxin and flavodoxin reductase have been described previously (*17*, *34*). *E. coli* strain BL21(DE3)pLysSpJJ15-4A overexpressing biotin synthase bearing a His_6 tag at its N-terminus (*35*) was a generous gift from Prof. J. Jarrett (University of Pennsylvania, Philadelphia, PA). Cells were cultivated and purified as described previously (*25*).

Preparation of Apoenzymes. Two methods of reduction using (a) 5-DAF and (b) sodium dithionite were employed.

(a) Solutions of 115 μM BS with 10 mM EDTA in 100 mM Tris-HCl (pH 8.0) (final concentrations) and 5-DAF (2.4 mM in DMSO), contained in separate Eppendorf tubes capped with airtight rubber septums, were degassed for 30 min at room temperature under a stream of moist argon. Using a gastight syringe, 5-DAF (final concentration of 24 μM) was added to give a final volume of 300 μL of the mixture. Photoreduction was initiated by irradiation with a white fluorescent tube (18 W) placed 10 cm away. After 1 h, the mixture was desalted on a PD-10 column (Pharmacia-Amersham) equilibrated with buffer and the enzyme concentrated on a Centricon 30 centrifugal filter device (Millipore).

(b) The following manipulations were performed inside the glovebox. A 100 mM solution of sodium dithionite was prepared in buffer, and its concentration was more precisely determined by titration with potassium ferricyanide. Aliquots (200 μL) of 150 μM BS were incubated with 30 equiv of

sodium dithionite for 90 min, during which the enzyme turned colorless. EDTA (30 equiv, stock solution of 100 mM) was then added and left for a further 60 min to chelate the free Fe^{2+}. The apoenzyme was then removed from the glovebox, desalted on a G-25 column, and concentrated using a Centricon 30 membrane concentrator.

The absence of [Fe-S] clusters in both preparations was verified by UV−visible spectroscopy. Aliquots of the apoenzymes were frozen in liquid nitrogen and stored at −80 °C until they were required.

Reconstitution of $[2Fe\text{-}2S]^{2+}$ and $[2Fe\text{-}2Se]^{2+}$ Centers into Apoenzymes. Aliquots (250 μL) of apo-biotin synthase (150 μM), 25 mM Na_2S in argon-saturated buffer, 25 mM $FeCl_3$, and 200 mM DTT (both dissolved in water) were deoxygenated in separate vials under a stream of moist argon for 30 min. After this time, using a gastight syringe, DTT was added to the apoenzyme to a final concentration of 5 mM and incubated for a further 30 min. A 6-fold excess of $FeCl_3$ and Na_2S were then added, and the reaction was allowed to proceed for 90 min after which EDTA (1 mM final concentration) was added and the mixture incubated for 30 min to chelate the free iron. The mixture was desalted on a PD-10 column equilibrated with buffer and concentrated to ≈240 μM on a Centricon 30 device. The $[2Fe\text{-}2Se]^{2+}$ enzyme was prepared using the same procedure except that Na_2Se replaced Na_2S. The stock solution of Na_2Se was diluted to a concentration of 25 mM with buffer in an Eppendorf tube, capped with an airtight septum before being removed from the glovebox just before use. The UV−visible spectra of the reconstituted S and Se enzymes were recorded, and their Fe content was determined. These enzymes were further concentrated on a Microcon YM-30 device to reach a minimum concentration of 3 mM for resonance Raman spectroscopy.

Reconstitution of $[4Fe\text{-}4S]^{2+}$ Centers into Apoenzymes. The apoenzyme (170 μL, 0.94 mM) and 200 μL aliquots of 40 mM $Fe(NH_4)_2(SO_4)_2$ or $FeCl_3$, 50 mM Na_2S, and 100 mM DTT were placed in separate 1.5 mL Eppendorf tubes and degassed under a continuous stream of moist argon for 30 min at ambient temperature before being introduced into the glovebox. The tubes were opened and then left to stand overnight at 16 °C. Before reconstitution, the sample volumes were remeasured to calculate the new concentrations to account for the evaporation that occurred overnight. DTT (10 mM) (*8*), or 5 mM when used with Fe^{3+} (*28*), was added to apo-BS, followed by a 6-fold excess of Fe^{2+} or Fe^{3+} and Na_2S. After 3 h, 2 mM EDTA (final concentration) was added. After 30 min, the sample was desalted on a PD-10 column. The reconstituted enzymes were concentrated with a Microcon YM-30 device inside the glovebox. Aliquots of the reconstituted enzymes were transferred to airtight cuvettes for determination of their UV−visible spectra. For resonance Raman analysis, they were directly frozen on the Raman sample holder inside the glovebox. Their Fe contents were also determined.

Enzymatic Assay. The assay has been described previously (*25*), but typically, it is realized in a final reaction volume of 100 μL and contained from 9 to 12 μM $[2Fe\text{-}2S]^{2+}$ BS, 100 μM DTB, 50 μM AdoMet, 2 mM NADPH, 2 μM flavodoxin, 0.05 μM flavodoxin reductase, 2 mM DTT, and 200 μM $Fe(NH_4)_2(SO_4)_2$ in 40 mM Tris buffer (pH 8.0). This was placed in a 1.5 mL septum-capped Eppendorf tube and was degassed for 10 min at room temperature by a continuous stream of moist argon until the red color, which appeared upon addition of Fe^{2+}, turned colorless. Then Na_2S (prepared in argon-saturated buffer) was added with a gastight syringe to give a final concentration of 100 μM. This mixture was left under argon for a further 15 min, followed by incubation at 37 °C for 4 h. Variants include substituting $[2Fe\text{-}2S]^{2+}$ BS with $[2Fe\text{-}2Se]^{2+}$ BS and Na_2S with Na_2Se (50 and 100 μM). After 4 h, the reaction was stopped by precipitation with 1% trichloroacetic acid and the mixture centrifuged at 13000*g* for 5 min at 4 °C, and the amount of biotin formed was determined on the supernatant by the paper disc-plate method using *L. plantarum* (*29*).

Verification by the resazurin test (*22*) showed that oxygen was still present after the 25 min incubation under argon. For the test, 100 μL of water left under the same conditions was introduced inside the glovebox and 100 μL of reduced resazurin was added. The water solution turned from colorless to pale pink, indicating the presence of traces of oxygen.

Quantification of Biotin and Selenobiotin. This was performed on 200 μL aliquots of the assay mixture. After proteins had been removed, the supernatant was loaded on a HPLC reversed phase C18 Nucleosil 100-5 Å, 250 mm × 4 mm column (Macherey-Nagel) equilibrated with 50 mM ammonium hydrogen phosphate (pH 2.6) and methanol (88:22 mixture). Absorbance was monitored at 200 nm. Under these conditions and at a flow rate of 1 mL/min, biotin eluted at ≈15 min and selenobiotin at ≈19 min. The selenobiotin:biotin ratio was determined from the areas of their respective HPLC peaks. A reference sample containing a mixture of both (prepared fresh) at a concentration of 5 μM each, run under identical conditions, served as a control. The selenobiotin:biotin ratio of the reference sample was consistently 1.05 ± 0.05.

Isolation of Selenobiotin for Mass Spectrometry. To avoid the presence of salts, the HPLC conditions were modified and were as follows [eluent A, H_2O with 0.05% TFA; and eluent B, H_2O with 0.05% TFA (50%) and CH_3CN (50%)]. Selenobiotin was eluted using a linear gradient from A to B of 100:0 to 20:80 over 25 min. The collected fractions were evaporated to dryness using a Speed Vac (Jouan) concentrator system.

Mass Spectrometry. Characterization of selenobiotin was performed using a MALDI-TOF mass spectrometer (MALDI-TOF-TOF, 4700 Proteomics, Applied Biosystems) in positive ion reflector mode. A saturated solution of α-cyano-4-hydroxycinnamic acid in CH_3CN and H_2O (0.1% TFA) (4:1, v/v) was used as a matrix. The recovered sample from HPLC was solubilized in 10 μL of a H_2O/MeOH mixture (1:1, v/v), and 0.5 μL was mixed with 2 μL of matrix. Then, 0.5 μL of the mixture (≈40 pmol) was deposited on the target. As a reference, 100 pmol of synthetic selenobiotin (*32*) was analyzed under the same conditions. The TOF mass spectrometer was tuned to give the highest resolution in the *m*/*z* 200−300 range, to allow the separation of selenobiotin ions from the chemical noise (matrix ions). All mass spectra were recorded using internal calibration.

Exchange Experiments of $[2Fe\text{-}2S]^{2+}$ BS and $[2Fe\text{-}2Se]^{2+}$ BS with Na_2Se and Na_2S, respectively. A mixture of 12 μM $[2Fe\text{-}2S]^{2+}$ BS or $[2Fe\text{-}2Se]^{2+}$ BS and 2 mM DTT in 40 mM Tris buffer (pH 8.0), in a final volume of 500 μL, was placed in a 1.5 mL septum-capped Eppendorf tube and was degassed

for 30 min at room temperature by a continuous stream of moist argon. DTT was added to the reaction mixture containing the $[2Fe\text{-}2Se]^{2+}$ enzyme to prevent its conversion to the apo form. Then, Na_2S (prepared in argon-saturated buffer) or Na_2Se diluted with buffer in the glovebox just before use was added with a gastight syringe to give a final concentration of 100 μM, and the mixture was left under argon for a further 30 min. The reaction mixture was incubated at 37 °C for 4 h, concentrated, and desalted on a Centricon 30 device before being analyzed by UV−visible spectroscopy. The isolated enzyme was further concentrated on a Microcon YM-30 device for analysis by resonance Raman spectroscopy.

Exchange Experiments of $[2Fe\text{-}2Se]^{2+}$ BS with Na_2S during the Enzymatic Reaction. The assays were performed as described above except that the volume of the reaction mixture was scaled up to 500 μL and concentrations of NADPH and flavodoxin were decreased to 1 mM and 1 μM, respectively, to minimize fluorescence interferences during resonance Raman measurements. For enzyme recovery, 10 Eppendorf tubes were employed. The reaction mixture was incubated at 37 °C for 30 min. At the end of this time, the contents from all the Eppendorf tubes were collected and 20 μL was saved for quantification on *L. plantarum*. The remaining fraction was desalted by being passed through Sephadex G-25 (the volume of the gel was 5 times that of the reaction mixture), concentrated, and further desalted with argon-saturated buffer by two rounds of a dilution−concentration process in a Centriprep 30 concentrator. The enzyme was analyzed by UV−visible spectroscopy and further concentrated using a Centricon device and a Microcon YM-30 device for resonance Raman spectroscopy.

Analytical Methods. The protein concentration was measured by the method of Bradford (*36*) using bovine serum albumin as a standard. BS concentrations were expressed per 41.3 kDa monomer (*35*). Iron was assayed by the method of Fish (*37*).

Spectroscopic Characterization. UV−visible spectra were recorded on a Uvikon 930 spectrophotometer (Kontron Instruments). Low-temperature (15 K) resonance Raman spectra were recorded using a modified Jobin-Yvon T64000 spectrometer equipped with a liquid nitrogen-cooled back-thinned CCD detector as described previously (*38*). The 457.9 nm line from an argon ion laser (Coherent Innova 90) used for Raman excitation did not exceed 100 mW at the sample. The spectral resolution was ≈3 cm^{-1}. Protein samples (1 μL, ≈3−6 mM) were deposited on a glass slide that was then transferred to a liquid helium optical cryostat. For air-sensitive proteins, samples were deposited onto a liquid nitrogen-cooled gold-plated copper disk contained in a glovebox and under a nitrogen atmosphere (<2 ppm O_2). The disk bearing the frozen protein sample was then quickly transferred to the optical cryostat. Baseline corrections were performed using GRAMS 32. No spectral smoothing was performed.

RESULTS

Characterization of $[2Fe\text{-}2Se]^{2+}$ Biotin Synthase. The procedure employed for the reconstitution of the $[2Fe\text{-}2S]^{2+}$ enzyme was applied to prepare the $[2Fe\text{-}2Se]^{2+}$ enzyme. The apo form was obtained by reduction of the as-isolated enzyme with either photoreduced 5-DAF (apoDAF) (*25*) or sodium dithionite (apoDT) (*7*, *26*). Apoenzymes prepared by photoreduction with 5-DAF could not be used for resonance Raman spectroscopy because they were fluorescent; consequently, almost all the experiments described herein were performed using enzymes reconstituted from apo forms obtained by reduction with dithionite except where mentioned. Reconstitution was effected in the presence of DTT and a 6-fold excess of $FeCl_3$ and Na_2Se, yielding an enzyme containing 2.1 ± 0.1 irons per monomer. A value of 2.9 ± 0.2 was found for the reconstituted $[2Fe\text{-}2S]^{2+}$ enzyme, suggesting the presence of nonspecific Fe in both reconstituted proteins. The UV−visible spectrum of the selenoenzyme exhibited absorption bands similar to those of the $[2Fe\text{-}2S]^{2+}$ enzyme, but they were less well-defined with lower absorbance values (Figure 1). For instance, the $[2Fe\text{-}2Se]^{2+}$ enzyme from three independent reconstitutions had an A_{452}/A_{280} ratio of 0.11 ± 0.01, whereas that of the as-isolated $[2Fe\text{-}2S]^{2+}$ enzyme is around 0.23, in accord with reported values of 0.21 ± 0.02 (*8*). The A_{452}/A_{280} ratio was 0.24 for the reconstituted $[2Fe\text{-}2S]^{2+}$ enzyme. The extinction coefficient values (ϵ) of native enzymes and selenoenzymes have been reported to be nearly the same (*39*); if this is also true for BS, a rough calculation indicates that only 50% of the cluster was reconstituted so that the rest of the added iron was probably nonspecific Fe.

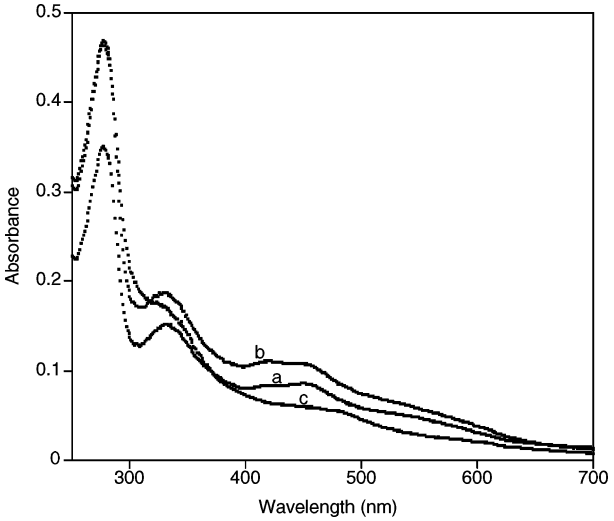

FIGURE 1: UV−visible absorption spectra of 12 μM biotin synthase in 50 mM Tris-HCl buffer (pH 8.0): (a) as-isolated $[2Fe\text{-}2S]^{2+}$ form, (b) reconstituted $[2Fe\text{-}2S]^{2+}$ form, and (c) reconstituted $[2Fe\text{-}2Se]^{2+}$ form.

The resonance Raman spectrum of the as-isolated form of BS (Figure 2a) clearly shows the presence of a $[2Fe\text{-}2S]^{2+}$ cluster; it is very similar (with respect to both relative band intensities and band frequencies) to that reported by Johnson and co-workers (*8*, *40*), who proposed tentative assignments for the observed bands. The relatively intense 301 cm^{-1} band has been assigned to the $B_{3u}{}^t$ mode, while that at 349 cm^{-1} was assigned to the $A_g{}^t$ mode. These two [Fe-S^t] stretching modes reflect modes primarily involving the terminal sulfur atoms of the three coordinating cysteine residues. Their relatively high frequencies reflect the incomplete cysteinyl coordination of the cluster (*40*) which has been confirmed by X-ray crystallography (*11*) with the identification of an arginine residue as the fourth coordinating ligand to the $[2Fe\text{-}2S]^{2+}$ cluster. The bands at 330, 366, 393, and 418 cm^{-1}

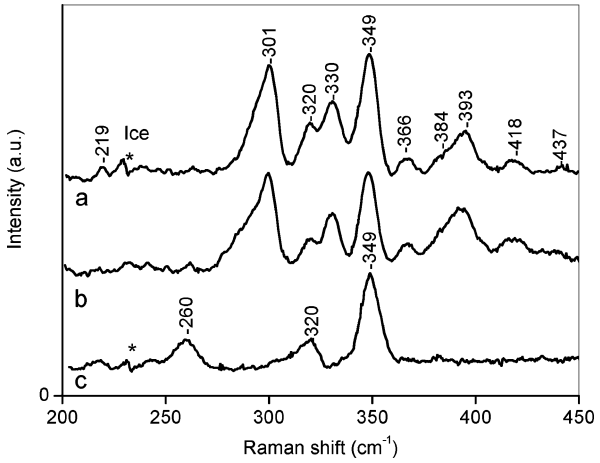

FIGURE 2: Low-temperature (15 K) resonance Raman spectra of biotin synthase in (a) the as-isolated $[2Fe\text{-}2S]^{2+}$ form, (b) the reconstituted $[2Fe\text{-}2S]^{2+}$ form, and (c) the reconstituted $[2Fe\text{-}2Se]^{2+}$ form. Enzyme concentrations were 1.5, 3.6, and 2.6 mM for spectra a−c, respectively, all in 50 mM Tris-HCl buffer (pH 8.0). Spectra were approximately normalized on the 349 cm^{-1} band. Spectra were recorded using 457.9 nm excitation with a laser power of 50 mW at the sample. Approximately 500 individual spectra with exposure times of 1−10 s were averaged. The resolution was ≈3 cm^{-1}. An asterisk indicates a residual from the subtraction of the ice contributions at 230 cm^{-1}.

Table 1: Observed Resonance Raman Bands (cm^{-1}) of Reconstituted $[2Fe\text{-}2Se]^{2+}$ Clusters in Biotin Synthase

$[2Fe\text{-}2Se]^{2+}$ BS	$[2Fe\text{-}2Se]^{2+}$ spinach ferredoxin[a]
217	220 (4.5)[b]
244?	231 (0.5)
260	261 (4.5)
–	272 (3)
320	328 (2.5)
349	355 (0)
–	369 (0)

[a] From Meyer et al. (*41*, *42*). [b] Values in brackets refer to $^{76}Se \rightarrow {}^{82}Se$ isotopic shifts.

have been assigned to [Fe-S^b] stretching modes involving primarily the bridging S^{2-} atoms (*8*, *40*). We note that Figure 2a exhibits a distinct band at 320 cm^{-1} which appears as a shoulder in the spectrum reported by Cosper et al. (*8*) and which was not tentatively assigned.

To validate the Se reconstitution procedure, we also prepared the $[2Fe\text{-}2S]^{2+}$ cluster, using the same method. Figure 2b represents the resonance Raman spectrum of reconstituted $[2Fe\text{-}2S]^{2+}$ BS; the similarity between this spectrum and that of the as-isolated protein indicates correct cluster reconstitution. Replacement of the elemental S^{2-} bridging atoms with the much heavier Se^{2-} atoms leads to a significant perturbation of the spectrum with the 330, 366, 393, and 418 cm^{-1} [Fe-S^b] bands being, as expected, the most affected (Figure 2c).

Reconstituted $[2Fe\text{-}2Se]^{2+}$ BS exhibits band frequencies that are similar to those reported for the reconstituted $[2Fe\text{-}2Se]^{2+}$ clusters in ferredoxins (*41*, *42*) (Table 1). However, the relative band intensities are different which could be due to the fact that the reconstituted $[2Fe\text{-}2Se]^{2+}$ clusters in the ferredoxins reported by Meyer et al. had complete cysteinyl coordination, which is not the case for biotin synthase. Isotopic $^{76}Se \rightarrow {}^{82}Se$ substitution measurements of the ferredoxin $[2Fe\text{-}2Se]^{2+}$ clusters led Meyer et al. to conclude,

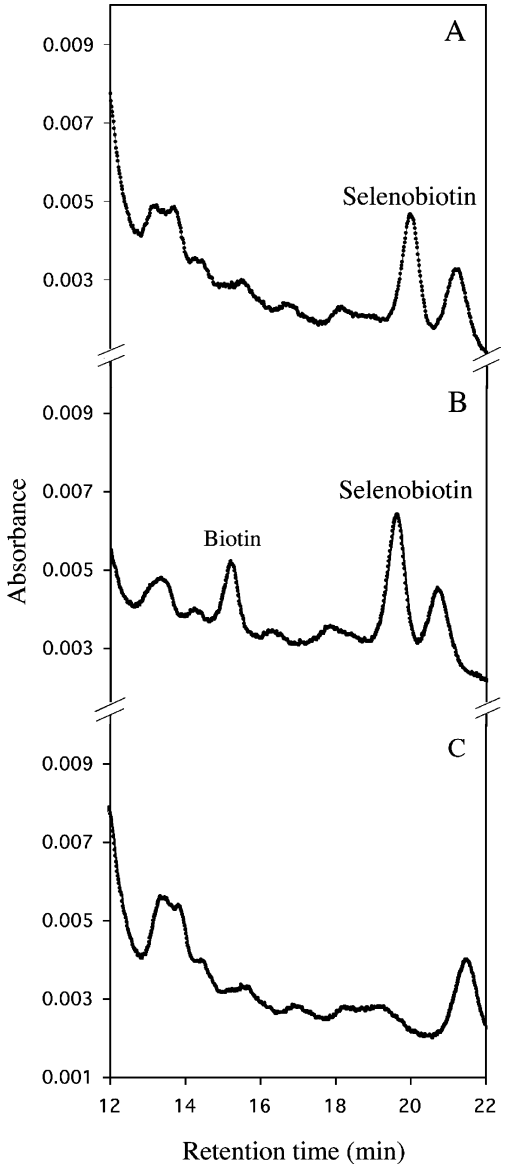

FIGURE 3: Chromatograms of reaction mixtures of (A) the standard assay as described in Materials and Methods containing 11 μM $[2Fe\text{-}2Se]^{2+}$ BS and 50 μM Na_2Se, (B) the standard assay performed with 11 μM $[2Fe\text{-}2Se]^{2+}$ BS and 50 μM Na_2S, and (C) the control, the standard assay performed with 11 μM $[2Fe\text{-}2Se]^{2+}$ BS and 50 μM Na_2Se without DTB. The column was a C18 Nucleosil 100-5 Å, 250 mm × 4 mm column, with a sample amount of 200 μL, a detection wavelength of 200 nm, a mobile phase of 50 mM ammonium hydrogen phosphate (pH 2.6) and methanol (88:22), and a flow rate of 1 mL/min.

on the basis of the lack of a shift of the 355 cm^{-1} band, that this mode is predominantly Fe−S(Cys) in character; this band corresponds to the one at 349 cm^{-1} in Figure 2c which indeed has been assigned to a terminal Fe−S(Cys) mode (*40*). Other bands, such as the 260 cm^{-1} band, were sensitive to $^{76}Se \rightarrow {}^{82}Se$ substitution and thus identify it as a [Fe-Se] mode (Table 1).

Under our Raman excitation conditions, the $[2Fe\text{-}2Se]^{2+}$ cluster is characterized by three distinct bands at 260, 320, and 349 cm^{-1}; however, resonance Raman bands at 320 and 349 cm^{-1} are also observed for the $[2Fe\text{-}2S]^{2+}$ cluster. It is important to note that above 350 cm^{-1}, no bands can beobserved for the $[2Fe\text{-}2Se]^{2+}$ cluster, whereas four bands at 366, 384, 393, and 418 cm^{-1} are clearly seen for the $[2Fe\text{-}2S]^{2+}$ cluster. These observations will be particularly useful

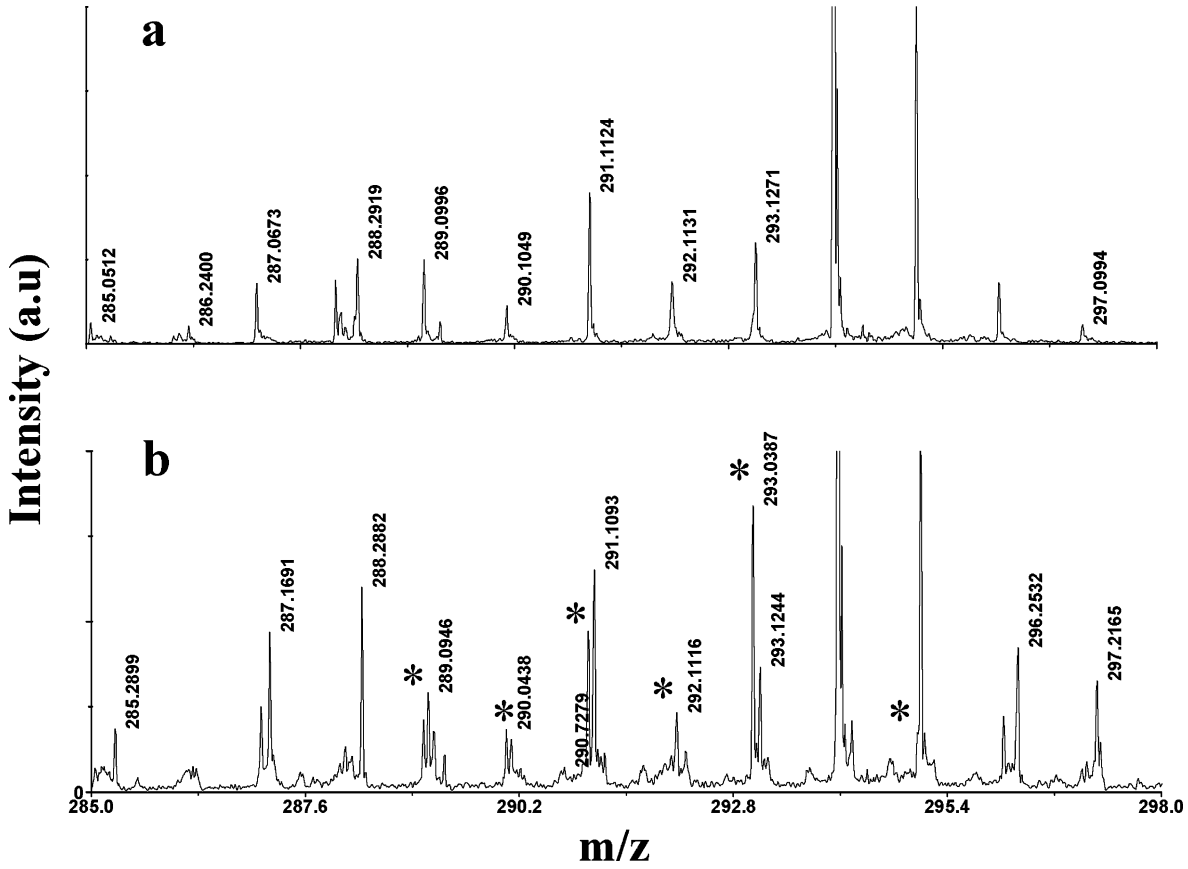

FIGURE 4: Partial positive ion MALDI-TOF mass spectra of the matrix (a) without and (b) with the fraction recovered from assay. Asterisks denote the most abundant selenobiotin isotopes (see Table 2).

for the identification and discrimination between the two clusters in the work described below.

Assay of [2Fe-2Se]$^{2+}$ Biotin Synthase. The [2Fe-2Se]$^{2+}$ enzyme was assayed in vitro under the standard conditions (*25*) in the presence of Na_2Se, instead of Na_2S, to allow the formation of a [4Fe-4Se]$^{2+}$ cluster. The reaction mixture, after removal of the proteins, was then analyzed by HPLC with a 50 mM ammonium hydrogen phosphate/methanol mixture as the eluent. A peak having the same retention time as a reference sample of selenobiotin, chemically synthesized in our laboratory (*32*), was observed (Figure 3A). Among all the HPLC conditions that were tested, this eluent was chosen because it allowed the best separation between selenobiotin and biotin (Figure 3B). However, for mass measurements, acetonitrile-trifluoroacetic acid was used instead, to avoid salt interference. The peak eluting at the same retention time as the reference selenobiotin, was collected and characterized by MALDI-TOF mass analysis. Although MALDI-TOF MS is mainly devoted to the analysis of large molecules ($m/z > 1000$), it has been found that this ionization process can also be used for detecting low-mass biotin and selenobiotin, even if interferences between the matrix signals cannot be ruled out. Among the various matrices tested, α-cyano-4-hydroxycinnamic acid was found to give the highest signal for biotin and selenobiotin. Due to the complex isotopic pattern of selenium, selenobiotin can be easily identified by the presence of the most abundant isotopes, as shown in Figure 4b. Table 2 shows the analysis of the signals expected for the protonated molecule of selenobiotin compared with those observed for the fraction recovered from the assay and synthetic selenobiotin, which served as a reference. It should be noted that no oxidized and no cationized forms of selenobiotin were detected for the fraction recovered from the assay. These results further identify the product formed in the assay as selenobiotin.

Table 2: Comparison of Expected and Experimental Values of Relative Abundances for the Different *m*/*z* Values of Protonated Selenobiotin (only the most abundant isotopes are indicated)

expected		synthetic (reference)		recovered from assay	
m/*z*	relative abundance (%)	*m*/*z*	relative abundance (%)	*m*/*z*	relative abundance (%)
289.043	18.38	289.044	19.9 ± 2	289.039	20.75 ± 3
290.044	17.41	290.043	17.6 ± 1	290.044	21.5 ± 2.5
291.043	49.38	291.045	50.0 ± 2	291.037	50.9 ± 2
292.046	5.98	292.04	5.9 ± 2	292.050	6.7 ± 2
293.040	100	293.035	100	293.039	100
294.043	12.17	294.04	12.5 ± 2	nd[a]	nd
295.041	18.83	295.043	17.1 ± 2	295.040	19.33 ± 2.5

[a] Nondetected ion due to interference with the matrix.

Selenobiotin was routinely quantified with *Lactobacillus plantarum* (*29*): selenobiotin standards responded exactly in the same way as biotin standards in the microbiological assay. Both biotin and selenobiotin were also quantified by HPLC using synthetic compounds injected under the same conditions, as standards. The values were in close agreement to those obtained using *Lactobacillus plantarum*. The difference did not exceed ± 5 %. This shows that the HPLC peaks were not contaiminated with impurities, as already suggested by the absence of peaks at the retention times of biotin and selenobiotin in the control experiment (Figure 3C).

Table 3: Turnover and Amounts of Biotin and Selenobiotin Obtained with the Different Types of BS[a]

entry	enzyme[b]	chalcogenide[c]	turnover[d]	HPLC[e] analysis selenobiotin:biotin ratio[f]
1	$[2Fe\text{-}2Se]^{2+}$	50 μM Na_2Se	0.13 ± 0.02	selenobiotin only
	from apoDT	100 μM Na_2Se	0.09 ± 0.03	nd[g]
2	$[2Fe\text{-}2Se]^{2+}$	50 μM Na_2Se	0.31 ± 0.04	selenobiotin only
	from apoDAF	100 μM Na_2Se	0.26 ± 0.04	nd[g]
3	$[2Fe\text{-}2Se]^{2+}$	50 μM Na_2S	0.32 ± 0.04	2.6 ± 0.44
	from apoDT	100 μM Na_2S	0.39 ± 0.04	2.1 ± 0.28
4	$[2Fe\text{-}2Se]^{2+}$	50 μM Na_2S	0.73 ± 0.14	1.1 ± 0.13
	from apoDAF	100 μM Na_2S	0.87 ± 0.06	0.86 ± 0.05
5	as-isolated	50 μM Na_2Se	0.42 ± 0.04	1.2 ± 0.0
	$[2Fe\text{-}2S]^{2+}$	100 μM Na_2Se	0.28 ± 0.06	1.9 ± 0.35
6	as-isolated	50 μM Na_2S	0.80 ± 0.01	nd[g]
	$[2Fe\text{-}2S]^{2+}$	100 μM Na_2S	0.98 ± 0.02	biotin only

[a] Data are means of three to six independent experiments. [b] The $[2Fe\text{-}2Se]^{2+}$ enzymes were reconstituted from apoenzymes, obtained by the reduction of the as-isolated forms with either sodium dithionite (apoDT) or 5-DAF (apoDAF). All enzymes were assayed as described in Materials and Methods, in the presence of the mentioned chalcogenide. [c] Concentrations of chalcogenides resulting in the best activities. [d] Moles of biotin or/and selenobiotin, as quantified by *L. plantarum*, per mole of BS monomer. [e] HPLC conditions: Nucleosil 100-5 C18 column, mobile phase of 50 mM ammonium hydrogen phosphate (pH 2.6) and methanol (88:22). [f] The selenobiotin:biotin ratio was determined from the areas of their respective HPLC peaks, as separated in Figure 3B. [g] Not determined.

The activity of the $[2Fe\text{-}2Se]^{2+}$ enzyme in the presence of 50 or 100 μM Na_2Se (larger amounts were inhibitory) was low; a turnover of $\approx$0.1 was obtained. Selenoenzymes reconstituted from apoenzymes issued from DAF reduction were more active, with a turnover of $\approx$0.3; but this value was lower than the usual turnover of $\approx$1 with the $[2Fe\text{-}2S]^{2+}$ enzyme and Na_2S (Table 3). This may be due to the intrinsic properties of both the $[2Fe\text{-}2Se]^{2+}$ and $[4Fe\text{-}4Se]^{2+}$ clusters. Assuming that the latter could be less efficient than the $[4Fe\text{-}4S]^{2+}$ cluster in the electron transfer, we replaced Na_2Se by Na_2S with the $[2Fe\text{-}2Se]^{2+}$ enzymes issued from both apoDAF and apoDT. Their turnovers were increased by approximately the same ratio, 3-fold, with the $[2Fe\text{-}2Se]^{2+}$ enzyme from apoDAF reaching $\approx$0.9 which is similar to that of the as-isolated enzyme in the presence of Na_2S (Table 3).

Analysis by HPLC of the assay mixture after reaction reveals the formation of a mixture of selenobiotin and biotin (Figure 3B). The presence of both products was quite unexpected if the $[2Fe\text{-}2S]^{2+}$ cluster is the sulfur donor (*7*, *21*−*23*). If one starts from $[2Fe\text{-}2Se]^{2+}$ BS, solely selenobiotin should have been produced, unless some S^{2-}/Se^{2-} exchange occurred within the $[2Fe\text{-}2Se]^{2+}$ center. As this could be due to the instability of the $[2Fe\text{-}2Se]^{2+}$ center, the reverse experiment starting from the as-isolated $[2Fe\text{-}2S]^{2+}$ enzyme and Na_2Se was performed. Again a mixture of biotin and selenobiotin was observed. The maximum turnover was $\approx$0.4 (Table 3).

State of the $[2Fe\text{-}2S(e)]^{2+}$ Cluster during Reaction. If the presence of the mixture of biotin and selenobiotin is due to a chalcogenide exchange in the $[2Fe\text{-}2S(e)]^{2+}$ cluster, both forms should be present simultaneously in the enzyme at some time during the course of the reaction. The $[2Fe\text{-}2Se]^{2+}$ enzyme was assayed in the presence of Na_2S for an arbitrary time of 30 min instead of the usual time of 4 h (*25*) to observe the state of the cluster during the course of reaction.

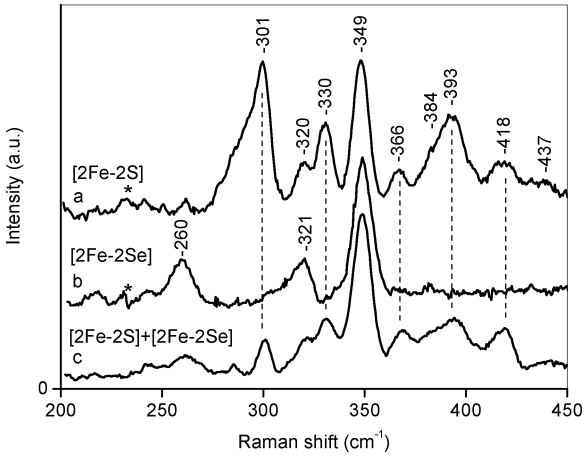

FIGURE 5: Low-temperature (15 K) resonance Raman spectra of biotin synthase in (a) the reconstituted $[2Fe\text{-}2S]^{2+}$ form (3.6 mM), (b) the reconstituted $[2Fe\text{-}2Se]^{2+}$ form (4.5 mM) before the assay, and (c) the reconstituted $[2Fe\text{-}2Se]^{2+}$ form (3.5 mM), isolated from the assay after a reaction time of 30 min. Same conditions as in Figure 2. The dashed lines highlight $[2Fe\text{-}2S]^{2+}$ cluster bands that have appeared in spectrum c.

The turnover was approximately 0.1. The reaction mixture was desalted by passing it through Sephadex G-25 equilibrated with argon-saturated buffer, concentrated, and further desalted to ensure the maximum elimination of cofactors that might cause fluorescence during resonance Raman measurement, by two rounds of the dilution−concentration process in a Centriprep 30 device. This procedure was successful since there was no interference of any fluorescence during resonance Raman analysis of the isolated enzyme. Both clusters were present (Figure 5c); this can be clearly seen when this spectrum is compared with the individual spectra of the $[2Fe\text{-}2S]^{2+}$ and $[2Fe\text{-}2Se]^{2+}$ clusters (parts a and b of Figure 5, respectively). The reaction was performed with the $[2Fe\text{-}2Se]^{2+}$ enzyme instead of the $[2Fe\text{-}2S]^{2+}$ enzyme because the $[2Fe\text{-}2Se]^{2+}$ spectrum exhibits no bands above 360 cm^{-1}, hence facilitating the identification of any newly formed $[2Fe\text{-}2S]^{2+}$ cluster which presents characteristic bands in the 360−450 cm^{-1} spectral range. In addition to the 260, 321, and 349 cm^{-1} bands of the initial $[2Fe\text{-}2Se]^{2+}$ cluster, Figure 5c clearly exhibits new bands at 366, (384), 393, 418, and 437 cm^{-1} which have been identified as those of the $[2Fe\text{-}2S]^{2+}$ cluster. The presence of the $[2Fe\text{-}2S]^{2+}$ cluster is signaled, furthermore, by a 301 cm^{-1} band in Figure 5c as well as by the 349 cm^{-1} band. We note that the relative intensity of the 349 cm^{-1} band in Figure 5c is significantly higher compared to that observed in Figures 5a and 5b. This observation further indicates that the 349 cm^{-1} band is common to both the $[2Fe\text{-}2S]^{2+}$ and $[2Fe\text{-}2Se]^{2+}$ clusters and that the spectrum in Figure 5c is clearly that of a mixture of both clusters.

In the assay, a $[4Fe\text{-}4S]^{2+}$ cluster should also be formed, but it was not detected on the isolated enzyme, purified under semianaerobic conditions. This could be due to its extreme sensitivity to oxygen (*8*, *26*, *28*, *35*) or to the fact that the resonance Raman signal of the $[4Fe\text{-}4S]^{2+}$ cluster is significantly lower than that of the $[2Fe\text{-}2S]^{2+}$ cluster under similar excitation conditions. The $[4Fe\text{-}4S]^{2+}$ cluster which served as a reference was prepared by reconstituting an apoenzyme with $Fe(NH_4)_2(SO_4)_2$ and Na_2S in the presence of DTT under strictly anaerobic conditions. Analysis by resonance Raman

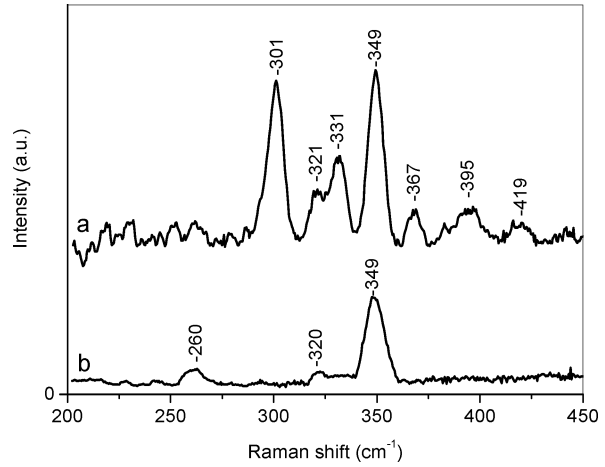

FIGURE 6: Low-temperature (15 K) resonance Raman spectra of biotin synthase isolated after an incubation time of 4 h: (a) as-isolated $[2Fe\text{-}2S]^{2+}$ BS incubated in the presence of Na_2Se and (b) reconstituted $[2Fe\text{-}2Se]^{2+}$ BS incubated in the presence of Na_2S and DTT. Enzyme concentrations were 6 and 4 mM, respectively. Same experimental conditions as in Figure 2.

spectroscopy showed that the Raman bands were similar to those of a $[4Fe\text{-}4S]^{2+}$ cluster, as published by Johnson's group (*8*). It should be noted that, in our hands, if the reconstitution was done with $FeCl_3$ instead of $Fe(NH_4)_2(SO_4)_2$, a mixture of $[4Fe\text{-}4S]^{2+}$ and $[2Fe\text{-}2S]^{2+}$ clusters was obtained, in contrast to what has been reported (*28*) (data not shown).

Importantly, no exchange occurred when either $[2Fe\text{-}2S]^{2+}$ BS or $[2Fe\text{-}2Se]^{2+}$ BS was incubated solely with Na_2Se or Na_2S, respectively, in 40 mM Tris buffer (pH 8.0). The incubation was performed as for a typical enzymatic assay at 37 °C for 4 h but with the omission of the other assay components. After 4 h, the $[2Fe\text{-}2Se]^{2+}$ enzyme was converted to the apo form as checked by UV−visible spectroscopy (spectrum not shown). Hence, the exchange experiment was repeated but this time with addition of 2 mM DTT. Analysis by resonance Raman spectroscopy (Figure 6) showed that there was no observable exchange between the clusters and the added chalcogenides. Overall, these results indicate that both the original $[2Fe\text{-}2S]^{2+}$ and reconstituted $[2Fe\text{-}2Se]^{2+}$ are stable as long as they are not solicited for reaction.

DISCUSSION

We provide here the first experimental proof that BS containing a $[2Fe\text{-}2Se]^{2+}$ cluster can produce selenobiotin in vitro. The standard in vitro assay of the native $[2Fe\text{-}2S]^{2+}$ enzyme is composed of DTB, AdoMet, NADPH, flavodoxin, flavodoxin reductase, DTT, Fe^{2+}, and Na_2S, the last two components being used to form the additional $[4Fe\text{-}4S]^{2+}$ cluster in situ. To investigate the selenium version of the reaction, we first replaced both [Fe-S] clusters with [Fe-Se] clusters. Thus, the $[2Fe\text{-}2Se]^{2+}$ enzyme was assayed in the presence of Na_2Se, to reconstitute a $[4Fe\text{-}4Se]^{2+}$ cluster. The $[2Fe\text{-}2Se]^{2+}$ enzyme was prepared by reconstituting the apoenzyme in the presence of DTT, $FeCl_3$, and Na_2Se, and the apo forms themselves were obtained from the native $[2Fe\text{-}2S]^{2+}$ enzyme, by reduction with either sodium dithionite (apoDT) or photoreduced 5-DAF (apoDAF). Both reconstituted selenoenzymes were tested in vitro. Analysis of the reaction mixture by HPLC showed the presence of a compound with the same retention time as synthetic selenobiotin (*32*), the nature of which was confirmed by mass spectrometry (Figure 4b). No biotin was formed. The turnovers, however, were much weaker than that of the $[2Fe\text{-}2S]^{2+}$ enzyme with Na_2S (turnover of ≈1), that is, ≈0.3 and ≈0.1 for the $[2Fe\text{-}2Se]^{2+}$ enzymes obtained from apoDAF and apoDT, respectively.

There could be several reasons for these lower activities.

(a) There is not enough $[2Fe\text{-}2Se]^{2+}$ or/and $[4Fe\text{-}4Se]^{2+}$ because the apoprotein is less efficiently reconstituted with Se^{2-} than with S^{2-}. Lower yields of $[2Fe\text{-}2Se]^{2+}$ clusters versus $[2Fe\text{-}2S]^{2+}$ clusters have already been reported, for example, in the assembly of spinach ferredoxin (*41*). The difference in the ionic radii of the two chalcogenides (Se is larger than S by ≈0.13 Å) might induce a less efficient folding of the polypeptide around the cluster (*31*). On the basis of the absorption properties of reconstituted $[2Fe\text{-}2Se]^{2+}$ BS, we estimated the amount of cluster to be in substoichiometric quantity (≈0.5 $[2Fe\text{-}2Se]^{2+}$). The amount of $[4Fe\text{-}4Se]^{2+}$ in the assay was not quantified, but the concentrations of added Fe^{2+} and Se^{2-} were optimized to produce the best activity.

(b) [Fe-Se] enzymes are more oxygen-sensitive than their corresponding sulfur counterparts (*31*). In our assay which contains traces of oxygen, as discussed in Materials and Methods, we know that the presence of DTT tends to preserve the $[2Fe\text{-}2Se]^{2+}$ cluster but we have no data related to the stability of the $[4Fe\text{-}4Se]^{2+}$ cluster. Since a turnover of 1 was obtained under these conditions with the $[2Fe\text{-}2S]^{2+}$ enzyme and Na_2S, this means that the $[4Fe\text{-}4S]^{2+}$ center is viable, but that might not be the case for the $[4Fe\text{-}4Se]^{2+}$ cluster.

(c) The reduction potentials of [Fe-S] and [Fe-Se] clusters are different. They vary from one protein to another and depend on a number of parameters. For instance, the hydrogen bond network surrounding the clusters is likely to be modified upon chalcogenide substitution in the [Fe-S(e)] clusters, and this is different in each protein (*31*). In our assay, the $[4Fe\text{-}4Se]^{2+}$ cluster might not be at the right redox potential to transfer electrons.

At this stage, however, it is extremely difficult to analyze the contribution of each factor, and we decided to simply investigate what would happen if we replace Na_2Se with Na_2S to form a mixed $[2Fe\text{-}2Se]^{2+}$ $[4Fe\text{-}4S]^{2+}$ enzyme. We observed that the activities of both $[2Fe\text{-}2Se]^{2+}$ BS increased by ≈3-fold and the selenoenzyme reconstituted from apoDAF could even reach a turnover of ≈1 (Table 3), which indicates that $[2Fe\text{-}2Se]^{2+}$ BS can function as well as $[2Fe\text{-}2S]^{2+}$ BS. However, the turnover of the $[2Fe\text{-}2Se]^{2+}$ enzyme reconstituted from apoDT was still not very high, ≈0.35. We have no straightforward explanation for the different activities between the two selenoenzymes, but it might be due to some subtle differences in the folded state of the apoenzymes obtained with the two reductants.

Interestingly, when the reaction mixture described above was analyzed, a mixture of selenobiotin and biotin was found. This result was quite unexpected since our recent observations (*22*), in agreement with those of other groups (*21*, *23*), strongly indicate that the $[2Fe\text{-}2S]^{2+}$ cluster is the sulfur source (either as the ultimate donor or via another intermediate), in which case solely selenobiotin would have been

formed. An exchange between the $[2Fe\text{-}2Se]^{2+}$ center and free S^{2-}, giving rise to a $[2Fe\text{-}2Se]^{2+}/[2Fe\text{-}2S]^{2+}$ mixture, could account for this result. Such an exchange of selenides with free sulfides has been reported in some [Fe-Se] centers; for instance, there was partial substitution of Se^{2-} with S^{2-} in the cluster of $[4Fe\text{-}4Se]^{2+}$ ferredoxin of *Clostridium pasteurianum*. On the other hand, there was no exchange with the $[4Fe\text{-}4S]^{2+}$ enzyme and free Se^{2-} (*43*). Biotin synthase could behave similarly; exchange occurring with the $[2Fe\text{-}2Se]^{2+}$ enzyme, whereas the $[2Fe\text{-}2S]^{2+}$ enzyme remained stable. To verify the last point, we carried out the reverse experiment in which we used the as-isolated $[2Fe\text{-}2S]^{2+}$ enzyme and Na_2Se. Again, a mixture of biotin and selenobiotin was formed. The turnover under these conditions was ≈0.4.

Thus far, we have not discussed the different selenobiotin:biotin ratios obtained in entries 3−5 of Table 3. For each entry, three to six independent experiments have been performed, leading to consistent values for selenobiotin and biotin quantification. Thus, the differences in the values of the selenobiotin:biotin ratio is not due to experimental uncertainty. At this stage, this variation is not easy to rationalize, but the important phenomenon is that a mixture of selenobiotin and biotin is always obtained when the two chalcogenides are present.

A possible explanation for the presence of this mixture might be that some exchange between free chalcogenides and those of the $[2Fe\text{-}2S(e)]^{2+}$ clusters had been taking place. If this were the case, we would be able to observe the simultaneous presence of a mixture of $[2Fe\text{-}2S]^{2+}$ and $[2Fe\text{-}2Se]^{2+}$ clusters in the enzyme. For reasons described above, resonance Raman spectroscopy was chosen for detection of the two clusters. Thus, $[2Fe\text{-}2Se]^{2+}$ BS was assayed in the presence of Na_2S for 30 min. As the assay contained several components, namely, AdoMet, NADPH, FMN in flavodoxin, and FAD in flavodoxin reductase, which might cause fluorescence during resonance Raman measurements, our major concern was to remove these potential interfering species during isolation of the enzyme. After the reaction, the enzyme was extensively desalted using Sephadex G-25 and Centriprep 30 concentrators. The isolated enzyme proved to be sufficiently nonfluorescent; besides the $[2Fe\text{-}2Se]^{2+}$ cluster, an additional $[2Fe\text{-}2S]^{2+}$ cluster was clearly observed in the resonance Raman spectrum (Figure 5c). In contrast, when either $[2Fe\text{-}2Se]^{2+}$ BS or $[2Fe\text{-}2S]^{2+}$ BS was incubated solely with Na_2S with DTT or Na_2Se, respectively, no exchange was observed (Figure 6a,b). We thus conclude that the exchange revealed in Figure 5c occurs only when there is reaction.

Jarrett's group showed by $^{56}Fe/^{57}Fe$ differential labeling that there was no exchange between free Fe and the Fe of the $[2Fe\text{-}2S]^{2+}$ cluster during reconstitution experiments with $FeCl_3$ and Na_2S; instead, the added Fe was incorporated into the protein to form a $[4Fe\text{-}4S]^{2+}$ cluster at a separate, distinct site (*10*). The presence of these two sites was later confirmed by the X-ray structure (*11*). Our results show that under similar conditions, the $[2Fe\text{-}2S(e)]^{2+}$ BS does not exchange with free chalcogenides. The two sets of experiments taken together imply that the $[2Fe\text{-}2S(e)]^{2+}$ cluster is quite stable. Examples in which both the Fe and the sulfide of the cluster can be easily exchanged with free iron and sulfide like in clostridial ferredoxins (*44*) and aconitase (*45*) exist in the literature, but apparently, this does not seem to be the case in BS. One possible reason might be that the $[2Fe\text{-}2S]^{2+}$ cluster is deeply buried inside the active site cleft (*11*), hence rendering it not easily accessible to solvent.

At this point, it is necessary to note that early studies have reported the conversion of $[2Fe\text{-}2S]^{2+}$ clusters to $[4Fe\text{-}4S]^{2+}$ clusters (*26*, *35*, *40*). To avoid confusion, it should be emphasized that this conversion occurs only when strong chemical reductants such as sodium dithionite and 5-DAF are used. The dissociation of the $[2Fe\text{-}2S]^{2+}$ cluster followed by a reassociation of iron into a $[4Fe\text{-}4S]^{2+}$ cluster was proposed as an explanation (*35*). However, as we recently showed by Mössbauer spectroscopy (*22*), once the active state containing a 1:1 mixture of $[2Fe\text{-}2S]^{2+}$ and $[4Fe\text{-}4S]^{2+}$ clusters is formed, the addition of the physiological reductant (NADPH, flavodoxin, and flavodoxin reductase) did not alter the clusters' proportions. It is only when DTB was introduced into the system that the amount of $[2Fe\text{-}2S]^{2+}$ cluster decreased. The amount of $[4Fe\text{-}4S]^{2+}$, whose function is to transfer an electron to AdoMet as mentioned above, remained unchanged. The latter observation renders very unlikely the possibility of any exchange of chalcogenides between the $[4Fe\text{-}4S(e)]^{2+}$ cluster and the $[2Fe\text{-}2Se(S)]^{2+}$ cluster during turnover. Therefore, the presence of a mixture of $[2Fe\text{-}2S]^{2+}$ and $[2Fe\text{-}2Se]^{2+}$ clusters (Figure 5c) is obviously due to the exchange of the selenide of $[2Fe\text{-}2Se]^{2+}$ BS with free sulfide. This exchange, as pointed out above, is strictly connected to the reaction process.

Thus, the production of selenobiotin and the presence of a mixture of $[2Fe\text{-}2Se]^{2+}$ $[2Fe\text{-}2S]^{2+}$ clusters in the assay containing $[2Fe\text{-}2Se]^{2+}$ BS and Na_2S provide additional evidence that the $[2Fe\text{-}2S(e)]^{2+}$ cluster is involved in the sulfur insertion step. However, the nature of the intermediates still remains to be clarified. Whether the $[2Fe\text{-}2S]^{2+}$ cluster is the ultimate sulfur donor has been recently discussed (*21*−*23*, *25*). Johnson and co-workers suggested that it could be a protein-bound sulfur resulting from the degradation of the cluster. This hypothesis cannot be completely excluded, but it should be supported by further experimental arguments. It relies on a published observation concerning aconitase, showing that persulfides could be generated in the apoprotein following [Fe-S] cluster degradation. This has been discussed in ref *25*, where we pointed out that in the cited work on aconitase, the apoprotein was obtained by oxidation with a large excess of ferricyanide but the biotin synthase assay is realized under strongly reducing conditions, in which case the presence of a persulfide is very unlikely. We still favor the first hypothesis, namely, the [2Fe-2S] center as the final donor. This makes sense since our mechanism implies that a carbon radical is trapped by the sulfur donor, which should possess a radical character. It is tempting to postulate the participation of the irons of the cluster in providing a radical reactivity to the inorganic sulfide. Work is in progress to provide further arguments.

To date, most examples of proteins in which the cluster sulfide has been replaced by selenide refer to ferredoxins (*31*), the function of which is to transfer electrons. The only example of which we are aware, concerning a true enzyme, is aconitase (*46*). With this study, we present a second example of an enzyme in which the [Fe-S] clusters were successfully substituted with [Fe-Se] clusters to yield an active homologue.

ACKNOWLEDGMENT

We thank Prof. J. Jarrett for the generous gift of the *E. coli* strain and T. Drujon for technical assistance.

REFERENCES

1. Sofia, H. J., Chen, G., Hetzler, B. G., Reyes-Spindola, J. F., and Miller, N. E. (2001) Radical SAM, a novel protein superfamily linking unresolved steps in familiar biosynthetic pathways with radical mechanisms: Functional characterization using new analysis and information vizualization methods, *Nucleic Acids Res. 29*, 1097−1106.
2. Marquet, A., Tse Sum Bui, B., and Florentin, D. (2001) Biosynthesis of biotin and lipoic acid, in *Vitamins and Hormones 61* (Litwack, G., and Begley, T., Eds.) pp 51−101, Academic Press, New York.
3. Marquet, A. (2001) Enzymology of carbon−sulfur bond formation, *Curr. Opin. Chem. Biol. 5*, 541−549.
4. Jarrett, J. T. (2005) The novel structure and chemistry of iron−sulfur clusters in the adenosylmethionine-dependent radical enzyme biotin synthase, *Arch. Biochem. Biophys. 433*, 312−321.
5. Lindblow-kull, C., Kull, F. J., and Shrift, A. (1980) Evidence for the biosynthesis of selenobiotin, *Biochem. Biophys. Res. Commun. 93*, 572−576.
6. Sanyal, I., Cohen, G., and Flint, D. H. (1994) Biotin synthase: Purification, characterization as a [2Fe-2S] cluster protein, and *in vitro* activity of the *Escherichia coli bioB* gene product, *Biochemistry 33*, 3625−3631.
7. Tse Sum Bui, B., Florentin, D., Fournier, F., Ploux, O., Méjean, A., and Marquet, A. (1998) Biotin synthase mechanism: On the origin of sulphur, *FEBS Lett. 440*, 226−230.
8. Cosper, M. M., Jameson, G. N. L., Hernandez, H. L., Krebs, C., Huynh, B. H., and Johnson, M. K. (2004) Characterization of the cofactor composition of *Escherichia coli* biotin synthase, *Biochemistry 43*, 2007−2021.
9. Ugulava, N. B., Gibney, B. R., and Jarrett, J. T. (2001) Biotin synthase contains two distinct iron−sulfur cluster binding sites: Chemical and spectroelectrochemical analysis of iron−sulfur cluster interconversions, *Biochemistry 40*, 8343−8351.
10. Ugulava, N. B., Surerus, K. K., and Jarrett, J. T. (2002) Evidence from Mössbauer spectroscopy for distinct $[2Fe\text{-}2S]^{2+}$ and $[4Fe\text{-}4S]^{2+}$ cluster binding sites in biotin synthase from *Escherichia coli*, *J. Am. Chem. Soc. 124*, 9050−9051.
11. Berkovitch, F., Nicolet, Y., Wan, J. T., Jarrett, J. T., and Drennan, C. L. (2004) Crystal structure of biotin synthase, an S-adenosylmethionine-dependent radical enzyme, *Science 303*, 76−79.
12. Nicolet, Y., and Drennan, C. L. (2004) AdoMet radical proteins−from structure to evolution−alignment of divergent protein sequences reveals strong secondary structure element conservation, *Nucleic Acids Res. 32*, 4015−4025.
13. Marsh, E. N. G., Patwardhan, A., and Huhta, M. S. (2004) S-Adenosylmethionine radical enzymes, *Bioorg. Chem. 32*, 326−340.
14. Layer, G., Heinz, D. W., Jahn, D., and Schubert, W.-D. (2004) Structure and function of radical SAM enzymes, *Curr. Opin. Chem. Biol. 8*, 468−476.
15. Birch, O. M., Fuhrmann, M., and Shaw, N. M. (1995) Biotin synthase from *Escherichia coli*, an investigation of the low molecular weight and protein components required for activity *in vitro*, *J. Biol. Chem. 270*, 19158−19165.
16. Ifuku, O., Koga, N., Haze, S., Kishimoto, J., and Wachi, Y. (1994) Flavodoxin is required for conversion of dethiobiotin to biotin in *Escherichia coli*, *Eur. J. Biochem. 224*, 173−178.
17. Guianvarc'h, D., Florentin, D., Tse Sum Bui, B., Nunzi, F., and Marquet, A. (1997) Biotin synthase, a new member of the family of enzymes which uses S-adenosylmethionine as a source of deoxyadenosyl radical, *Biochem. Biophys. Res. Commun. 236*, 402−406.
18. Shaw, N. M., Birch, O. M., Tinschert, A., Venetz, V., Dietrich, R., and Savoy, L.-A. (1998) Biotin synthase from *Escherichia coli*: Isolation of an enzyme-generated intermediate and stoichiometry of S-adenosylmethionine use, *Biochem. J. 330*, 1079−1085.
19. Ollagnier-de-Choudens, S., Sanakis, Y., Hewitson, K. S., Roach, P., Münck, E., and Fontecave, M. (2002) Reductive cleavage of S-adenosylmethionine by biotin synthase from *Escherichia coli*, *J. Biol. Chem. 277*, 13449−13454.
20. Escalettes, F., Florentin, D., Tse Sum Bui, B., Lesage, D., and Marquet, A. (1999) Biotin synthase mechanism: Evidence for hydrogen transfer from the substrate into deoxyadenosine, *J. Am. Chem. Soc. 121*, 3571−3578.
21. Ugulava, N. B., Sacanell, C. J., and Jarrett, J. T. (2001) Spectroscopic changes during a simgle turnover of biotin synthase: Destruction of a [2Fe-2S] cluster accompanies sulfur insertion, *Biochemistry 40*, 8352−8358.
22. Tse Sum Bui, B., Benda, R., Schünemann, V., Florentin, D., Trautwein, A. X., and Marquet, A. (2003) Fate of the $[2Fe\text{-}2S]^{2+}$ cluster of *Escherichia coli* biotin synthase during reaction: A Mössbauer characterization, *Biochemistry 42*, 8791−8798.
23. Jameson, G. N. L., Cosper, M. M., Hernandez, H. L., Johnson, M. K., and Huynh, B. H. (2004) Role of the [2Fe-2S] cluster in recombinant *Escherichia coli* biotin synthase, *Biochemistry 43*, 2022−2031.
24. Ollagnier-de Choudens, S., Mulliez, E., Hewitson, K. S., and Fontecave, M. (2002) Biotin synthase is a pyridoxal phosphate-dependent cysteine desulfurase, *Biochemistry 41*, 9145−9152.
25. Tse Sum Bui, B., Lotierzo, M., Escalettes, F., Florentin, D., and Marquet, A. (2004) Further investigation on the turnover of *Escherichia coli* biotin synthase with dethiobiotin and 9-mercaptodethiobiotin as substrates, *Biochemistry 43*, 16432−16441.
26. Tse Sum Bui, B., Florentin, D., Marquet, A., Benda, R., and Trautwein, A. X. (1999) Mössbauer studies of *Escherichia coli* biotin synthase: Evidence for reversible interconversion between $[2Fe\text{-}2S]^{2+}$ and $[4Fe\text{-}4S]^{2+}$ clusters, *FEBS Lett. 456*, 411−414.
27. Tse Sum Bui, B., Escalettes, F., Chottard, G., Florentin, D., and Marquet, A. (2000) Enzyme-mediated sulphide production for the reconstitution of [2Fe-2S] clusters into apo-biotin synthase of *Escherichia coli*. Sulphide transfer from cysteine to biotin, *Eur. J. Biochem. 459*, 2688−2694.
28. Ollagnier-de-Choudens, S., Sanakis, Y., Hewitson, K. S., Roach, P., Baldwin, J. E., Münck, E., and Fontecave, M. (2000) Iron−sulfur center of biotin synthase and lipoate synthase, *Biochemistry 39*, 4165−4173.
29. Izumi, Y., Osakai, M., and Yamada, H. (1987) Biotin assay using lyophilized and glycerol-suspended cultures, *J. Microbiol. Methods 6*, 237−246.
30. Sommen, G., Comel, A., and Kirsch, G. (2003) Substituted selenophenes starting from ketene dithioacetals and sodium selenide, *Synlett 6*, 855−857.
31. Meyer, J., Moulis, J.-M., Gaillard, J., and Lutz, M. (1992) Replacement of sulfur by selenium in iron−sulfur proteins, *Adv. Inorg. Chem. 38*, 73−115.
32. Bory, S., and Marquet, A. (1976) Synthèse de la (+) sélénobiotine, *Tetrahedron Lett.*, 2033−2036.
33. Lacourciere, G. M., Mihara, H., Kurihara, T., Esaki, N., and Stadtman, T. C. (2000) *Escherichia coli* NifS-like proteins provide selenium in the pathway for the biosynthesis of selenophosphate, *J. Biol. Chem. 275*, 23769−23773.
34. Sanyal, I., Gibson, K. J., and Flint, D. H. (1996) *Escherichia coli* biotin synthase: An investigation into the factors required for its activity and its sulfur donor, *Arch. Biochem. Biophys. 326*, 48−56.
35. Ugulava, N. B., Gibney, B. R., and Jarrett, J. T. (2000) Iron−sulfur cluster interconversions in biotin synthase: Dissociation and reassociation of iron during conversion of [2Fe-2S] to [4Fe-4S] clusters, *Biochemistry 39*, 5206−5214.
36. Bradford, M. M. (1976) A rapid and sensitive method for the quantification of microgram quantities of protein using the principle of protein-dye binding, *Anal. Biochem. 72*, 248−254.
37. Fish, W. W. (1998) Rapid colorimetric micromethod for the quantitation of complexed iron in biological samples, *Methods Enzymol. 158*, 357−364.
38. Mathé, C., Nivière, V., and Mattioli, T. A. (2005) Fe^{3+}-hydroxide ligation in the superoxide reductase from *Desulfoarculus baarsii* is associated with pH dependent spectral changes, *J. Am. Chem. Soc. 127*, 16436−16441.
39. Fee, J. A., Mayhew, S. G., and Palmer, G. (1971) The oxidation−reduction potentials of parsley ferredoxin and its selenium-containing homolog, *Biochim. Biophys. Acta 245*, 196−200.
40. Duin, E. C., Lafferty, M. E., Crouse, B. R., Allen, R. M., Sanyal, I., Flint, D. H., and Johnson, M. K. (1997) [2Fe-2S] to [4Fe-4S] cluster conversion in *Escherichia coli* biotin synthase, *Biochemistry 36*, 11811−11820.

41. Meyer, J., Moulis, J.-M., and Lutz, M. (1986) High-yield chemical assembly of [2Fe-2X] (X = S, Se) clusters into spinach apoferredoxin: Product characterization by resonance Raman spectroscopy, *Biochim. Biophys. Acta 871*, 243−249.

42. Meyer, J., Moulis, J.-M., and Lutz, M. (1986) Resonance Raman spectroscopy of $[2Fe\text{-}2X]^{2+}$ (X = S, Se) clusters in ferredoxins, *Biochim. Biophys. Acta 873*, 108−118.

43. Moulis, J.-M., and Meyer, J. (1982) Characterization of the selenium-substituted 2[4Fe-4Se] ferredoxin from *Clostridium pasteurianum*, *Biochemistry 21*, 4762−4771.

44. Hong, J.-S., and Rabinowitz, J. C. (1970) Base-catalyzed exchange of the iron and sulfide of clostridial ferredoxin, *J. Biol. Chem. 245*, 6582−6587.

45. Kennedy, M. C., Emptage, M. H., and Beinert, H. (1984) Incorporation of [^{35}S]sulfide into the Fe−S cluster of aconitase, *J. Biol. Chem. 259*, 3145−3151.

46. Breton, J. L., Farrar, J. A., Kennedy, M. C., Beinert, H., and Thomson, A. J. (1995) Magnetic circular dichroism study of the selenium-substituted form (Fe_3Se_4) of bovine heart aconitase, *Biochem. J. 311*, 197−202.

BI052388M